SHC 2013, International Conference on Solar Heating and Cooling for Buildings and Industry
September 23-25, 2013, Freiburg, Germany

Mass flow, pressure drop, and leakage dependent modeling and characterization of solar air collectors

Christian Welz[a,1], Christoph Maurer[a], Paolo Di Lauro[a], Gerhard Stryi-Hipp[a], Michael Hermann[a]

[a]*Fraunhofer Institute for Solar Energy Systems ISE, Heidenhofstraße 2, 79110 Freiburg, Germany*

Abstract

In comparison to liquid collectors, the thermal efficiency of air collectors strongly depends on the mass flow, and often air collectors can be leaky. Further, for efficient system operation, the air collector's mass flow will be chosen regarding the auxiliary power demand of the fan caused by the pressure drop of the system. In this work the interdependency between thermal and hydraulic behavior and the resulting primary energy demand will be explained. Moreover, suitable mass flow dependent models for thermal efficiency, pressure drop and leakage will be presented. Because of the mass flow dependent correlation of the thermal power gain and the auxiliary power demand, a novel characterization method for air collectors will be proposed considering both.

Selection and peer review by the scientific conference committee of SHC 2013 under responsibility of PSE AG.

Keywords: solar; air collector; air heater; mass flow; pressure drop; leakage; modeling; characterization; system

1. Comparison of liquid and air collectors regarding mass flow dependency

The differences of air and liquid collectors lead to individual preferences within a diversity of applications in buildings, agriculture, and industry as well as different climates. Decision factors may be the demanded kind of heated fluid, the necessity of storage, the space requirement for tubes, the risk of leaking liquid, stagnation, and the maintenance effort. Distinct construction principles and fluids and their different influence on heat transfer and transport occur.

Many air collectors have the advantage of a low thermal resistance from the absorbing surface through the thin absorber sheet to reach the fluid surface, whereas in liquid heating collectors the heat must be conducted to the fluid surface along a much longer path with a smaller cross section (Fig. 1). Liquid collectors benefit from the fluid properties, which cause a small convective thermal resistance between the tube-liquid surface into the liquid. Air collectors instead have a much higher convective thermal resistance between the channel-air surface into the air due to air properties. The fact that air collectors often have heat conducting ribs attached to the absorber for enlarging the convective air surface is neglected in this schematic consideration.

The convective thermal resistance depends inversely on the mass flow. In liquid collectors the convective thermal resistance takes just a small part of the resistance from the absorbing surface into the liquid stream. Therefore, the thermal efficiency of liquid collectors does not much depend on the mass flow, and high thermal efficiencies can be reached even with low mass flow rates. Thus, the electrical auxiliary energy demand for the pump can be kept small. Therefore, simple thermal efficiency models of liquid collectors do not consider the mass flow. In air collectors the convective thermal resistance makes the bigger share of the resistance from the absorbing surface into the air stream. Thus, the thermal efficiency has a high mass flow dependency. For high thermal efficiencies high mass flows with an accompanying high electrical auxiliary energy demand of the fan blowing through the whole system must be chosen. Thermal efficiency and mass flow will be balanced ecologically or economically.

[1] Corresponding author. Tel.: +49-761-4588-5869; fax: +49-761-4588-9950.
E-mail address: christian.welz@ise.fraunhofer.de

Nomenclature

a_1	coefficient for temperature dependent heat loss, W/(m²K)
a_2	coefficient for quadratic temperature dependent heat loss, W/(m²K²)
$a_{1_{max}}$	coefficient for temperature dependent heat loss at infinite mass flow, W/(m²K)
$a_{2_{max}}$	coefficient for quadratic temperature dependent heat loss at infinite mass flow, W/(m²K²)
a_3	coefficient for mass flow dependent heat loss, s/kg
A_{Field}	aperture area of collector field, m²
$\dot{C}_{\substack{Auxiliary\ Consumption \\ of\ Solar\ System}}$	instantaneous electrical energy costs per time caused by fan or pump of the solar system, $, €, …
$\dot{C}_{\substack{Saved\ Consumption \\ of\ Convential\ System}}$	saved instantaneous combustible costs per time of the conventional system, $, €, …
C_{Eff}	specific heat capacity per collector area, J/(kgKm²)
c_p	specific heat capacity, J/(kgK)
$d_{1_e,1_i}$	linear coefficient for measured leakage mass flow (*e* = exit, *i* = inlet), kg/sPa
$d_{2_e,2_i}$	quadratic coefficient for measured leakage mass flow (*e* = exit, *i* = inlet), kg/sPa²
F'_0	collector efficiency factor at ΔT = 0, 1
$F'_{0_{max}}$	collector efficiency factor at ΔT = 0 and infinite mass flow (maximum of F'$_0$), 1
G	global irradiance on collector field plane, W/m²
G_{dif}	diffuse irradiance on collector field plane, W/m²
G_{dir}	direct (beam) irradiance on collector field plane, W/m²
h_1	linear pressure drop coefficient, Pas/kg
h_2	quadratic pressure drop coefficient, Pas²/kg²
k_{dif}	incidence angle modifier for diffuse irradiance, 1
k_{dir}	incidence angle modifier for direct (beam) irradiance, 1
$\dot{m}$	mass flow, kg/s
$\dot{m}_{ave,Row}$	average mass flow of serial collectors in one row, kg/s
$\dot{m}_{\substack{ave,Row \\ cLoop}}$	average mass flow in collector field for closed loop, kg/s
$\dot{m}_{\substack{ave,Row \\ L_e,L_i \\ oLoop}}$	average mass flow in collector field for open loop (L_e = leaving leakage, L_i = entering leakage), kg/s
$\dot{m}_i$	mass flow of collector field at inlet, kg/s
$\dot{m}_e$	mass flow of collector field at outlet, kg/s
$\dot{m}_{\substack{L_e,L_i \\ Meas \\ Coll}}$	measured leakage mass flow of one collector not flown through (*e* = exit, *i* = inlet), kg/s
$\dot{m}_{L_e,L_i}$	calculated leakage mass flow of collector field flown through (*e* = exit, *i* = inlet), kg/s

$\dot{m}_{\substack{Le \\ Subs}}$	substitution mass flow (*oLoop* = for open loop, *cLoop* = for closed loop), kg/s
$n_{Coll\,/\,Row}$	number of serial collectors in one row, 1
$n_{Coll\,/\,Field}$	number of collectors per field, 1
n_{Row}	number rows of collector field, 1
p	inner collector pressure, Pa
p_i	inner collector field pressure at inlet, Pa
p_e	inner collector field pressure at outlet, Pa
$P_{\substack{Auxiliary\ prim.\ Power \\ Solar\ System}}$	instantaneous primary auxiliary power used by fan or pump of the solar system, W
$P_{\substack{Net\ prim.\ Power \\ Coll.}}$	instantaneous saving of net primary power , W
$\dot{P}_{Net\ profit}$	instantaneous net profit per time, $, €, …
$P_{\substack{Therm.\ Power \\ Coll.}}$	saved conventional instantaneous primary power of the conventional system, W
$\dot{Q}_{L_i}$	power loss caused by the entering leakage mass flow, W
$\dot{Q}_{L_e}$	power loss caused by the leaving leakage mass flow, W
$\dot{q}_{Cap}$	power absorbed by thermal capacitance of collector field related to field area and to 0 °C, W/m²
$\dot{q}_{\substack{L_e \\ 0°C}}$	power loss caused by leaving leakage mass flow and related to field area and to 0 °C, W/m²
$\dot{q}_{\substack{L_i \\ 0°C}}$	power loss caused by entering leakage mass flow and related to field area and to 0 °C, W/m²
$\dot{q}_{\substack{e \\ 0°C}}$	power leaving the collector field at outlet related to field area and to 0 °C, W/m²
$\dot{q}_{\substack{i \\ 0°C}}$	power entering the collector field at inlet related to field area and to 0 °C, W/m²
$\dot{q}_{Gain}$	power gain (enthalpy flow, collector capacitance) of leaking collector field related to field area, W/m²
t	point of time (0 = at initial point of time, 1 = at following point of time), s
T_a	ambient temperature, °C
T_i	fluid temperature at collector field inlet, °C
T_e	fluid temperature at collector field outlet, °C
T_m	mean fluid temperature (t_0 = at initial point of time, t_1 = at following point of time), °C
U_0	heat transfer coefficient from absorber to ambient, W/(m²K)
U_1	coefficient for temperature dependent heat transfer from absorber to ambient, W/(m²K²)
Δp	pressure drop of collector field, Pa
ΔT	difference of mean fluid temperature and ambient temperature, K
η	instantaneous collector efficiency, 1
η_0	conversion factor, 1

$\eta_{0_{max}}$	conversion factor at infinite mass flow, 1
$(\tau\alpha)_e$	effective transmittance-absorptance product (i.e. effective optical efficiency), 1

An additional issue is that air collectors can be leaky. This can cause thermal losses depending on the component order in the air loop. Leakage also influences the internal average mass flow of air collectors, which again affects the thermal efficiency. One determining parameter of leakage is the mass flow.

Because of the mass flow dependency of air collectors, this article provides mass flow dependent models for thermal efficiency, pressure drop, and leakage. From these models the energy balance will be set up to calculate the air temperature at the collector outlet. Finally a method for finding an appropriate individual mass flow for air collectors and the subsequent graphical characterization will be proposed.

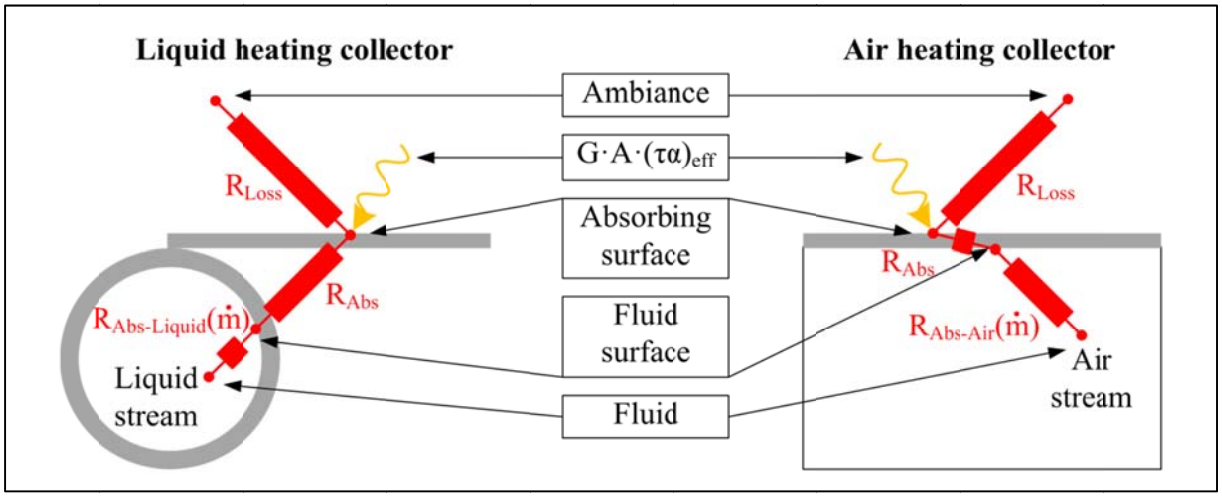

Fig. 1. The contrasting juxtaposition of the main thermal resistances in a liquid and an air heating collector shows the dominant mass flow dependent resistance from the fluid surface into the fluid stream of the air collector.

2. Thermal efficiency model

For a good comparability of parameters the thermal efficiency model for liquid collectors (1) was extended.

$$\eta(\Delta T/G) = \eta_0 - a_1 \cdot \frac{\Delta T}{G} - a_2 \cdot \frac{\Delta T^2}{G} \tag{1}$$

with

$$\Delta T = (T_i + T_e)/2 - T_a \tag{2}$$

and with the collector parameters (with changes from [1])

$$\eta_0 = (\tau\alpha)_e \cdot F'_0 \qquad a_1 = F'_0 \cdot U_0 \qquad a_2 = F'_0 \cdot U_1 \tag{3}$$

The collector efficiency factor *F'* depends on the thermal resistance between the absorbing surface and the fluid stream, whose mass flow dependency will be considered as

$$F'_0(\dot{m}) = F'_{0_{max}} \cdot f(\dot{m}) \tag{4}$$

The empirical exponential function (5) was proved suitable. If leakage will be considered, the mass flow is the average mass flow along a collector or a collector row (see chapter 4.7). The parameter a_3 describes the mass flow dependent heat loss. This is caused by the mass flow dependent convective heat transfer characteristics influencing the temperature of the absorber leading to the heat loss.

$$f(\dot{m}) = 1 - e^{-a_3 \cdot \dot{m}_{ave,Row}} \tag{5}$$

Equation (5) set in (4), (3), and eventually in (1) becomes

$$\eta(\Delta T/G, \dot{m}) = \left[1 - e^{-a_3 \cdot \dot{m}_{ave,Row}}\right] \cdot \left[\eta_{0_{\max}} - a_{1_{\max}} \cdot \frac{\Delta T}{G} - a_{2_{\max}} \cdot \frac{\Delta T^2}{G}\right] \tag{6}$$

Fig. 2 shows on the left side the efficiency curves of a flat plate air collector at three different mass flows according to model (1). On the right side the mass flow dependent efficiency surface of the same collector according to model (6) is shown. Both models were fitted by use of the same measurement points indicated in the diagrams. Henceforth, with model (6) simulation with an infinitely variable mass flow within the measured mass flow range is possible. Analysis on extrapolation within turbulent flow showed good agreement. Since laminar flow has a different physical-thermal behavior, extrapolation into the transition region and the laminar region leads to exorbitant high model errors. For more details on extrapolation analysis see [2].

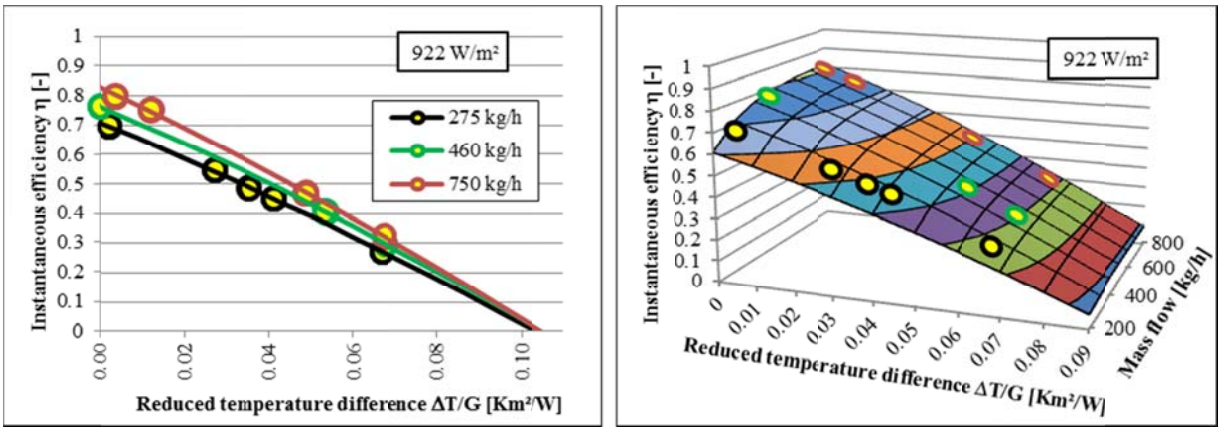

Fig. 2. Left: Efficiency curves of an air collector at three different mass flows according to model (1).
Right: Mass flow dependent efficiency surface of the same collector according to model (6).

3. Pressure drop model

For turbulent flow pressure drop is a function in-between linear and quadratic dependency of flow velocity. Therefore a second order polynomial suits well for the mass flow dependent modeling of the pressure drop of collectors. The pressure drop of a row of collectors (serial connection) (7) equals the product of the number of collectors in row and the pressure drop of one collector.

$$\Delta p(\dot{m}) = n_{Coll/Row} \cdot \left(h_1 \cdot \dot{m} + h_2 \cdot \dot{m}^2\right) \tag{7}$$

4. Leakage model

4.1. Measurement

For measuring the leaving and the entering leakage mass flow, the air collector fluid connections are sealed, and the collecter is exposed to overpressure or underpressure respectively through an additionally connected thin hose. The pressure-dependent mass flow to maintain the pressure is then measured and considered as leaving and entering leakage mass flow. Leakage of one air collector is well described with a second order polynomial (8). For overpressure d_{1e} and d_{2e} are the coefficients and for underpressure the coefficients are d_{1i} and d_{2i} respectively. Examples of the leakage curves for overpressure and underpressure are displayed in Fig. 3. The possible different leakage trends visible in the diagram lead to the definition of individual curves for overpressure and underpressure respectively.

$$\dot{m}_{\substack{L_e,L_i \\ Meas \\ Coll}}(p) = d_{1_e,1_i} \cdot p + d_{2_e,2_i} \cdot p^2 \tag{8}$$

4.2. Types of circuits

For leakage modeling it is useful to distinguish three system configuration cases:

- Open loop with overpressure
- Open loop with underpressure
- Closed loop with overpressure and underpressure

The pressure developments of these cases are shown in Fig. 3. The green arrows from the collectors to the pressure curve of the closed loop point out that significant pressure differences and therefore leakage mass flows occur among the single collectors. The other two system cases lead to even higher pressures and leakage mass flows. The pressure difference to ambient will increase further if additional components cause additional pressure drop in the open loops. In the closed loop leaving and entering leakage occur simultaneously.

The following developed leakage models do consider all this, since they are set up for a rectangular collector field of several rows in width and several collectors in length. For theoretical investigations rational numbers (not only integer) are possible for the number of rows and the number of collectors in row. The consideration of the whole collector field in the leakage model simplifies the calculation significantly compared to the calculation of every single collector in the field.

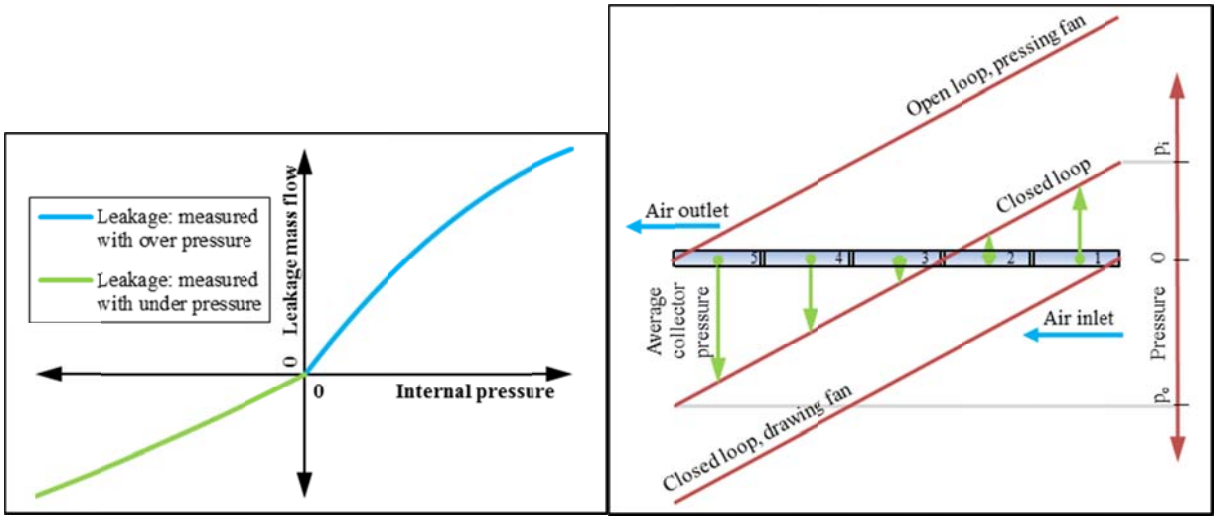

Fig. 3. Left: Measured pressure dependent leakage curves of an air collector according to equation (8).
Right: Leakage determining pressure curves (red) in a collector field for the three system cases.

The modeling underlies the assumption of the uniform distribution of the leakage openings along the air collector field. The influence of possible flow distortions at the interconnections of the air collectors is not considered in the pressure drop calculation. For the closed loop it is assumed additionally that except for the collector field there is no further leakage in the loop. The model always requires the outlet mass flow, since usually this mass flow shall cover a preset user demand.

4.3. Pressure

Initially the pressures at the inlet and the outlet of the collector field must be obtained. For the open loop with overpressure the pressure at the outlet arises from the system. The pressure at the inlet is achieved by

$$p_i = p_e + \Delta p \tag{9}$$

For the open loop with underpressure the pressure at the inlet arises from the system as well. The pressure at the outlet is achieved by

$$p_e = p_i - \Delta p \tag{10}$$

Due to unequal leakage mass flows for overpressure and underpressure, as can be seen in Fig. 3 (left), the pressure calculation is more complex for the closed loop. The pressure at the inlet can be found by use of equation (15) and by the second root (zero of a function) of a cubic function, which is

$$p_i = t - \frac{b}{3a} \tag{11}$$

with

$$t = 2\sqrt{-\frac{p'}{3}} \cdot \cos\left[\frac{1}{3}\arccos\left(\frac{3q'}{2p'}\sqrt{\frac{-3}{p'}}\right) - \frac{2\pi}{3}\right] \tag{12}$$

with

$$p' = \frac{3ac - b^2}{3a^2} \qquad q' = \frac{2b^3 - 9abc + 27a^2d}{27a^3} \tag{13}$$

with

$$\begin{aligned} a &= \frac{d_{2_e}}{3} - \frac{d_{2_i}}{3} & b &= \frac{d_{1_e}}{2} - \frac{d_{1_i}}{2} + d_{2_i} \cdot \Delta p \\ c &= d_{1_i} \cdot \Delta p - d_{2_i} \cdot \Delta p^2 & d &= -\frac{d_{1_i}}{2} \cdot \Delta p^2 + \frac{d_{2_i}}{3} \cdot \Delta p^3 \end{aligned} \tag{14}$$

Equation (11) is not usable, if for the curves of measured leakage mass flow (8) only linear coefficients are available. For this case the author found another solution not published yet. Another possibility may be to use very small quadratic coefficients in (8), which will lead to errors without significance.

The pressure at the outlet is calculated with equation (10).

4.4. Leakage mass flow

For establishing the models of leakage mass flow, it is necessary to set up and solve an integral and include the different boundary conditions of the three system cases. After solving the integral for all three system cases the universal model is found.

$$\dot{m}_{L_e,L_i} = \frac{n_{Coll\,/\,Field}}{\Delta p} \cdot \left[\frac{d_{1_e,1_i}}{2} \cdot \left(p_i^2 - p_e^2\right) + \frac{d_{2_e,2_i}}{3} \cdot \left(p_i^3 - p_e^3\right)\right] \tag{15}$$

Here, equations (7) and (9), (10), or (11) are necessary. For the leakage mass flow of the open loop with overpressure and of the overpressure zone of the closed loop the coefficients d_{1e} and d_{2e} must be used. For the overpressure zone of the closed loop p_e is set to zero additionally. A leakage mass flow with a positive algebraic sign will be achieved.

For the leakage mass flow of the open loop with underpressure and of the underpressure zone of the closed loop the coefficients d_{1i} and d_{2i} must be used. For the underpressure zone of the closed loop p_i is set to zero additionally. A leakage mass flow with a negative algebraic sign will be achieved.

4.5. Leakage power loss

The power loss caused by the leaving leakage mass flow of the open and the closed loop is

$$\dot{Q}_{L_e} = \dot{m}_{\underset{Subs}{L_e}} \cdot c_p \cdot \left(T_e - T_i\right) \tag{16}$$

Leaving powers are handled with positive algebraic signs and entering powers with negative algebraic signs within the whole modeling, because the useful power at the outlet is a leaving power and has to become positive. Therefore, the leakage power loss of a field caused by overpressure will be achieved with a positive algebraic sign for the common case of $T_i < T_e$.

In (16) $\dot{m}_{L_e,Subs}$ represents a substitution mass flow, which does not exist in reality. It results from considering the increasing air temperature between the inlet and the outlet of the air collector field. A linear increasing temperature of the leakage mass flow along the air collector field is considered in the calculation of the thermal

energy transport by leaking air, where (16) results with the substitution mass flow after integration over the collector field length. For the open loop with overpressure the substitution mass flow is

$$\dot{m}_{\substack{L_e \\ Subs \\ oLoop}} = \frac{n_{Coll\,/\,Field}}{\Delta p^2} \cdot \left[\begin{array}{l} \frac{d_{1e}}{2} \cdot p_i \cdot \left(p_i^2 - p_e^2 \right) \\ + \left(-\frac{d_{1e}}{3} + \frac{d_{2e}}{3} \cdot p_i \right) \cdot \left(p_i^3 - p_e^3 \right) \\ -\frac{d_{2e}}{4} \cdot \left(p_i^4 - p_e^4 \right) \end{array} \right] \tag{17}$$

For the overpressure zone of the closed loop p_e is set to zero, and the substitution mass flow results in

$$\dot{m}_{\substack{L_e \\ Subs \\ cLoop}} = \frac{n_{Coll\,/\,Field}}{\Delta p^2} \cdot \left[\frac{d_{1e}}{6} \cdot p_i^3 + \frac{d_{2e}}{12} \cdot p_i^4 \right] \tag{18}$$

When this leakage power loss (16) becomes related to the field area and the temperature point of 0 °C (for convenient use of temperatures with the unit degree Celsius in the model), it follows

$$\dot{q}_{\substack{L_e \\ 0°C}} = \frac{\dot{m}_{\substack{L_e \\ Subs}} \cdot c_p}{A_{Field}} \cdot \left(T_e - T_i \right) + \frac{\dot{m}_{L_e} \cdot c_p}{A_{Field}} \cdot T_i \tag{19}$$

The power loss caused by the entering leakage mass flow of the open and the closed loop is

$$\dot{Q}_{L_i} = \dot{m}_{L_i} \cdot c_p \cdot \left(T_a - T_i \right) \tag{20}$$

This power loss comes along with a positive algebraic sign for the common case of $T_i > T_a$. For the open loop with underpressure often $T_i = T_a$. Then this power loss will be zero.

When this leakage power loss becomes related to the field area and the temperature point of 0 °C, it follows

$$\dot{q}_{\substack{L_i \\ 0°C}} = \frac{\dot{m}_{L_i} \cdot c_p}{A_{Field}} \cdot T_a \tag{21}$$

4.6. Inlet mass flow

To use the modeled collector field in a system model, the inlet mass flow must be known. Since outgoing mass flows come along with a positive algebraic sign, ingoing mass flows carry a negative algebraic sign. This makes it easier to add the leakage model to existing collector models. The inlet mass flow of the open loop with overpressure is

$$\dot{m}_i = -\dot{m}_e - \dot{m}_{Le} \tag{22}$$

The inlet mass flow of the open loop with underpressure is

$$\dot{m}_i = -\dot{m}_e - \dot{m}_{Li} \tag{23}$$

The inlet mass flow of the closed loop with overpressure and underpressure is

$$\dot{m}_i = -\dot{m}_e \tag{24}$$

4.7. Average mass flow

It was identified that the change of the main mass flow caused by leakage, which was used in the thermal efficiency model (6), influences the thermal power in a similar dimension as the leakage does. Therefore it is

appropriate to quantify this mass flow change and to consider it in the thermal efficiency model. In order to do this the average mass flow of one row is necessary. For both variations of the open loop this is

$$\dot{m}_{\substack{ave,Row \\ L_e,L_i \\ oLoop}} = \frac{\dot{m}_e}{n_{Row}} - \frac{n_{Coll/Field}}{n_{Row}\cdot\Delta p}\cdot\left[\frac{d_{1_e,1_i}}{2}\cdot p_e^2 + \frac{d_{2_e,2_i}}{3}\cdot p_e^3\right] + \frac{n_{Coll/Field}}{n_{Row}\cdot\Delta p^2}\cdot\left[\frac{d_{1_e,1_i}}{6}\cdot\left(p_i^3 - p_e^3\right) + \frac{d_{2_e,2_i}}{12}\cdot\left(p_i^4 - p_e^4\right)\right] \tag{25}$$

For the average mass flow of one row in an open loop with overpressure the coefficients d_{1e} and d_{2e} will be used. For the open loop with underpressure the coefficients d_{1i} and d_{2i} will be used.

The average mass flow of one row in the closed loop is

$$\dot{m}_{\substack{ave,Row \\ cLoop}} = \frac{\dot{m}_e}{n_{Row}} + \frac{n_{Coll/Field}}{n_{Row}\cdot\Delta p^2}\cdot\left(-\frac{d_{1_e}}{3}\cdot p_i^3 - \frac{d_{2_e}}{4}\cdot p_i^4 + \frac{d_{1_i}}{3}\cdot p_e^3 + \frac{d_{2_i}}{4}\cdot p_e^4\right) \tag{26}$$

5. Energy balance

5.1. Energy balance

For simulation it is necessary to write the energy balance and to calculate the outlet temperature of the collector field for each time step. With consideration of the leakage power losses, the thermal collector capacity, and its values with its algebraic signs the energy balance related to the field area is

$$\dot{q}_{Gain} = \dot{q}_{\substack{e \\ 0°C}} + \dot{q}_{\substack{Le \\ 0°C}} + \dot{q}_{\substack{i \\ 0°C}} + \dot{q}_{\substack{Li \\ 0°C}} + \dot{q}_{Cap} \tag{27}$$

The entering and leaving specific power and the specific heat flow caused by the thermal capacity are

$$\dot{q}_{\substack{e \\ 0°C}} = \frac{\dot{m}_e\cdot c_p}{A_{Field}}\cdot T_e \qquad \dot{q}_{\substack{i \\ 0°C}} = \frac{\dot{m}_i\cdot c_p}{A_{Field}}\cdot T_i \qquad \dot{q}_{Cap} = C_{Eff}\cdot\frac{T_{m_{t_1}} - T_{m_{t_0}}}{t_1 - t_0} \tag{28}$$

at which T_m is the mean fluid temperature.

Setting the specific powers (19), (21) and (28) into the energy balance (27) and rearranging it becomes to

$$\dot{q}_{Gain} = \frac{\left(\dot{m}_e + \dot{m}_{\substack{L_e \\ Subs}}\right)\cdot c_p}{A_{Field}}\cdot\left(T_e - T_i\right) + \frac{\dot{m}_{L_i}\cdot c_p}{A_{Field}}\cdot\left(T_a - T_i\right) + C_{Eff}\cdot\frac{T_{m_{t_1}} - T_{m_{t_0}}}{t_1 - t_0} \tag{29}$$

5.2. Outlet temperature

For the analytical calculation of the outlet temperature the left side of (29) will be replaced by the product of thermal efficiency (6) and the area specific global solar irradiance. For $\eta_{0,max}$ in (6) the beam and the diffuse irradiance will be considered together with its incidence angle modifiers. After rearranging this quadratic equation to a general quadratic function the outlet temperature will be achieved with the second root (zero of a function) by

$$T_e = \frac{-b + \sqrt{b^2 - 4ac}}{2a} \tag{30}$$

at which under consideration of equation (5)

$$a = \frac{a_{2\max} \cdot f(\dot{m})}{2}$$

$$b = \frac{a_{1\max} \cdot f(\dot{m})}{2} + a_{2\max} \cdot f(\dot{m}) \cdot (T_i - 2 \cdot T_a) + \frac{\left(\dot{m}_e + \dot{m}_{L_{e\,Subs}}\right) \cdot c_p}{A_{Field}} + \frac{C_{Eff}}{2 \cdot (t_1 - t_0)}$$

$$\begin{aligned} c = & -\eta_{0\max} \cdot f(\dot{m}) \cdot (k_{dir} \cdot G_{dir} + k_{dif} \cdot G_{dif}) \\ & + \frac{a_{1\max} \cdot f(\dot{m})}{2} \cdot (T_i - 2 \cdot T_a) + \frac{a_{2\max} \cdot f(\dot{m})}{2} \cdot (T_i - 2 \cdot T_a)^2 \\ & - \frac{\left(\dot{m}_e + \dot{m}_{L_{e\,Subs}}\right) \cdot c_p}{A_{Field}} \cdot T_i + \frac{\dot{m}_{L_i} \cdot c_p}{A_{Field}} \cdot (T_a - T_i) + \frac{C_{Eff}}{2 \cdot (t_1 - t_0)} \cdot (T_i - 2 \cdot T_{m_{t_0}}) \end{aligned} \quad (31)$$

5.3. Plausibility check of energy balance including entire leakage model

A validation of the model parts in chapter 4 and the energy balance of chapter 5.1 with measurement results were not done, since a test sample with uniform distribution of leakage and a high effort of precise measurement equipment would be necessary.

The entire leakage model in chapter 4 was tested thoroughly for plausibility in a spreadsheet numerically and graphically. Measurement data of pressure drop and leakage were used for the model inputs.

Afterwards the entire leakage model and the energy balance were implemented in the widely-used collector type 832 v3.08 for TRNSYS in a type version which is not yet publically available, and it runs in simulations. Simulation results were compared with spreadsheet results with exact agreement. The determination of the outlet temperature was not implemented into type 832. Instead, its original iterative solution was left unchanged.

6. Determination of an ecologic or economic mass flow

Chapter 6 and 7 give an overview of the determination of an ecologic or economic mass flow and characterization of collectors with the consideration of these mass flows. Details on the methodology can be found in [3].

6.1. Mass flow of Maximum saving of Primary power, MMP (ecologic mass flow)

The MMP is defined as the collector mass flow which is necessary for the instantaneous maximum saving of net primary power of the conventional system by the solar system. The net primary power saving is defined as the difference in (32). The minuend is the saved conventional instantaneous power of the conventional system, which equals the thermal energy production of the collector. The subtrahend is the instantaneous primary power used by the fan or pump of the solar system. The subtrahend considers the conversion factor from primary power to the hydraulic power supply of the fan or pump, which is identical to the hydraulic power demand of the whole solar system including the collector field.

$$P_{\substack{Net\ prim.\ Power \\ Coll.}} = P_{\substack{Therm.\ Power \\ Coll.}} - P_{\substack{Auxiliary\ prim.\ Power \\ Solar\ System}} \quad (32)$$

Currently the primary energy factor, the thermal efficiency of the conventional system, and the thermal losses of the solar system other than thermal losses of the collector field are neglegted in the minuend. These are relatively small and compensate for each other partly in (32). Storage losses and a low degree of utilization are not considered also.

6.2. Mass flow of Maximum saving of operating Costs, MMC (economic mass flow)

The MMC is defined as the collector mass flow which is necessary for the instantaneous maximum net profit per time. The net profit per time is defined as the difference in (33). The minuend is the saved instantaneous energy costs per time of the conventional system by the solar system. The subtrahend is the instantaneous electrical energy costs per time caused by the fan or pump of the solar system. Both terms consider energy prices.

$$\dot{P}_{Net\ profit} = \dot{C}_{\substack{Saved\ Consumption \\ of\ Convential\ System}} - \dot{C}_{\substack{Auxiliary\ Consumption \\ of\ Solar\ System}} \tag{33}$$

The following is valid for both, the MMP and the MMC: A smaller mass flow can be used in case the user's power demand is smaller than the solar system's power output. This will save auxiliary energy or costs and raise the coefficient of performance COP. A higher mass flow is never advisable. A higher mass flow would increase the auxiliary power or costs effort faster than the thermal power gain or the saved combustible costs. If the user's power demand is larger than the solar system's power output, it is advised to run the solar system ecologically or economically and to add supplementary power as much as needed.

For (32) and (33) the flow resistance of the solar system without the collector field and of the collector field must be known. The first is assumed to be constant with the precondition of a sizable solar system. The latter will be determined by the product of the flow resistance of one collector and the number of collectors in row. For the mass flow determination methods the number of rows of the collector field is not necessary to know, even if collectors in whole systems are considered, as long as the fan or pump efficiency is assumed to be constant instead of volume flow dependent.

6.3. Determination of MMP and MMC

Two methods to find the MMP or the MMC have been developed. One uses simulation or measurement points. The other one is based on curve models for thermal power and flow resistance. Both methods find the mass flows by setting the first derivative of (32) or (33) with respect to mass flow to zero if previously made mass flow dependent.

The determination method using simulation or measurement points is applied in Fig. 4 for a physically simulated covered flat plate air collector with black absorber. The thermal power of the vacuum tube is showed by the continuous blue curve (minuend of (32)). The red curve shows the primary power used by the fan to flow trough the whole system including the vacuum tube (subtrahend of (32)). The dotted blue curve shows the net power (difference of (32)), where the maximum needs to be found. Therefore three simulation points near the possible maximum become fitted by a quadratic function shown as green curve. With the first derivative set equal to zero the MMP is found shown as green cross. The procedure can become repeated for different operating conditions and system flow resistances.

For the method using curve models model (6) can be a base part of the minuend of (32), and equation (7) can be a base part of the subtrahend of (32). The left side of (32), the net primary power saving, is shown in the 3D diagram for the same air collector. The yellow curve follows the ridge (maximum for each reduced temperature difference) of the net power surface, where the MMP can be read out for different operating conditions.

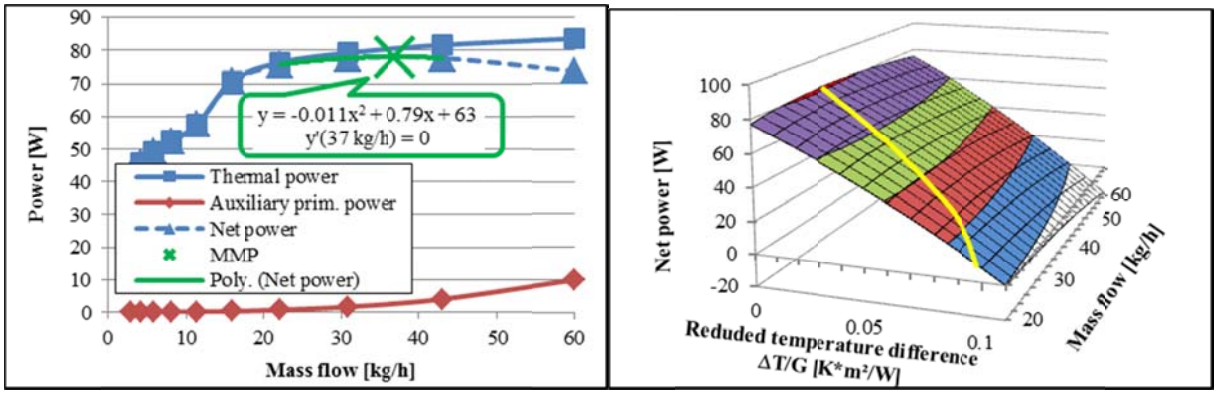

Fig. 4. Determination of MMP for a covered flat plate air collector with black absorber by using simulation points (left) and curve models (right).

7. Characterization of collectors with consideration of mass flow

After the determination of the MMP or the MMC using simulation or measurement points corresponding reduced temperature differences can be calculated (Fig. 5, left upper diagram). For the simulation or measurement points of the instantaneous efficiency, of the primary energetic coefficients of performance (COP), and of the temperature raises quadratic functions can be fitted. By using these functions for interpolation, these three variables can be determined for each identified MMP or MMC. The results are displayed in Fig. 5 for the covered flat plate air collector. It shows the characteristics of the air collector performing in three systems with

different flow resistances while operated ecologically in each shown point. To avoid misunderstanding, the COP_{prim} must be multiplied by the primary energy factor of electricity to get the common COP_{end}. At this state collectors can be distinguished by comparing their performance considering flow resistance of system and collector and thermal behavior of the collector.

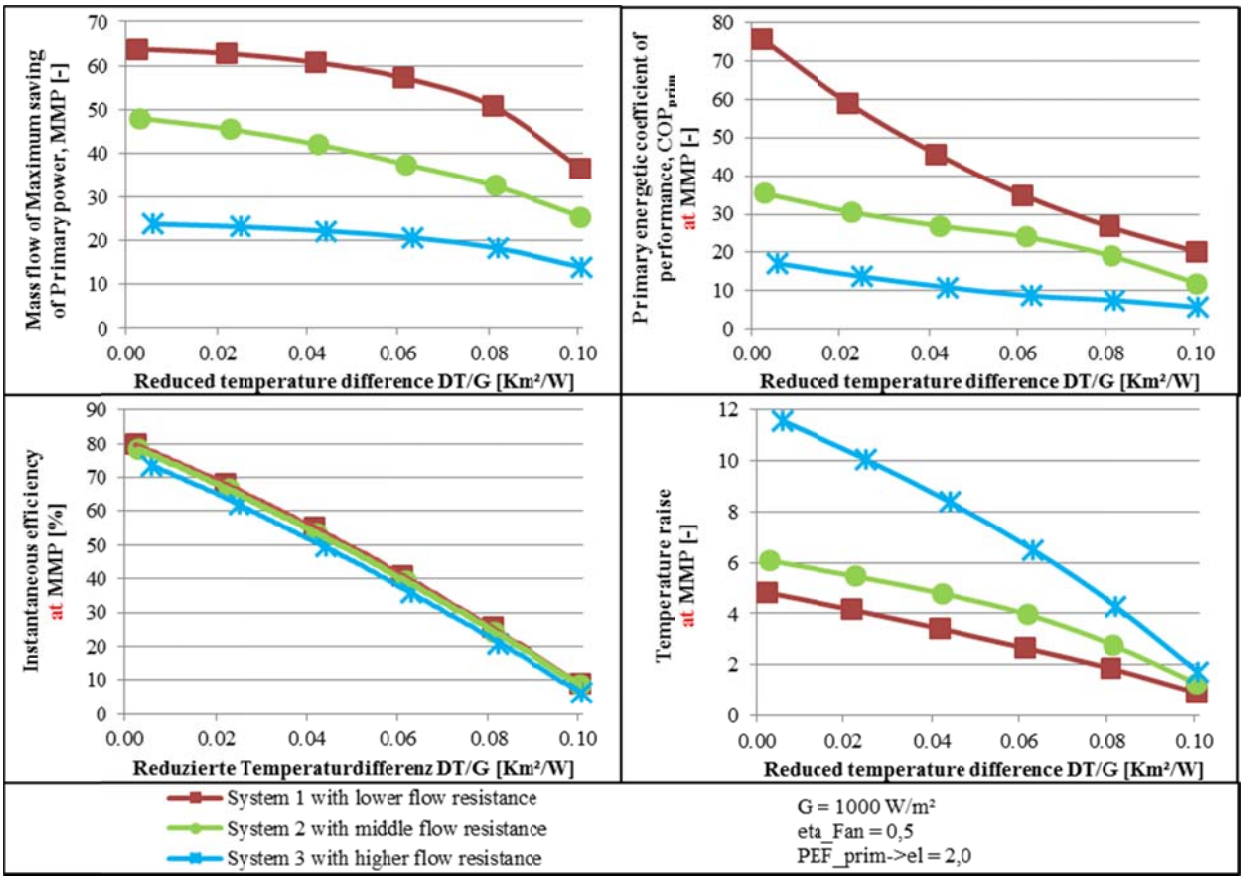

Fig. 5. Characteristic variables of a covered flat plate air collector with black absorber considering the flow resistance of three systems and the collector and the thermal behavior of the collector.

8. Conclusion

In this work a simple mass flow dependent thermal efficiency model for collectors was built which allows simulations with an infinitely variable mass flow. Further the leakage of air collectors was modeled in detail and can be considered in simulations. The new models are implemented in the TRNSYS type 832.

Methods for determining ecologic and economic mass flows of mass flow dependent collectors were established, thus the Mass flow of Maximum saving of Primary power MMP and the Mass flow of Maximum saving of operating Costs MMC can be found. Subsequent this enables the described characterization and comparison of mass flow dependent collectors in the system context.

Acknowledgements

The project Cost-Effective (support code: NMP2-LA-2008-212206) was funded by the EU's Seventh Framework Programme for Research. The project Luko-E (support code: 0325959A) was funded by the German Federal Ministry for the Environment, Nature Conservation and Nuclear Safety.

References

[1] Perers B. An improved dynamic solar collector test method for determination of non-linear optical and thermal characteristics with multiple regression. Solar Energy, Volume 59, Issues 4–6, April–June 1997, Pages 163–178. http://dx.doi.org/10.1016/S0038-092X(97)00147-3

[2] Welz C, Di Lauro P, Thoma C, Richter J, Hermann M, Stryi-Hipp G, Maurer C. Physikalische Modellierung und Simulation sowie detaillierte Vermessung von Luftkollektoren. Proceedings 22. Symposium „Thermische Solarenergie", Bad Staffelstein. Germany, 2012.

[3] Welz C, Knecht M, Di Lauro P, Maurer C, Stryi-Hipp G, Hermann M. Thermohydraulische Simulation von Luftkollektoren und Luftkollektorsystemen und Systembezogene Bewertung von Luftkollektoren. Proceedings 23. Symposium „Thermische Solarenergie“, Bad Staffelstein. Germany, 2013.